

Study on Electronic and Optical Properties of Graphene Oxide Under an External Electric Field From First-principles

Abdehafid Najim

Sultan Moulay Slimane University: Universite Sultan Moulay Slimane

Omar BAJJOU (✉ bajjou.omar@gmail.com)

Sultan Moulay Slimane University: Universite Sultan Moulay Slimane <https://orcid.org/0000-0003-0346-3847>

Mustapha BOULGHALLAT

Universite Sultan Moulay Slimane de Beni-Mellal

Mohammed Khenfouch

Ibn Zohr University: Universite Ibn Zohr

Khalid Rahmani

University Sultan Moulay Slimane of Beni-Mellal: Universite Sultan Moulay Slimane de Beni-Mellal

Research Article

Keywords: External electric field, Optical property, First-principle calculation, electronic structure, absorption spectrum

Posted Date: November 3rd, 2021

DOI: <https://doi.org/10.21203/rs.3.rs-996018/v1>

License:  This work is licensed under a Creative Commons Attribution 4.0 International License.

[Read Full License](#)

Study on electronic and optical properties of graphene oxide under an external electric field from first-principles

Abdelhafid NAJIM¹, Omar BAJJOU^{2*}, Mustapha BOULGHALLAT¹, Mohammed KHENFOUCH^{3,4}, Khalid RAHMANI⁵.

¹*LDD, Faculty of Sciences and Technics, Sultan Moulay Slimane University, BP 523, 23000 Morocco, najim.phymo@gmail.com.*

²*Material Physics Laboratory, Faculty of Sciences and Technics, Sultan Moulay Slimane University, BP 523, 23000 Beni Mellal, Morocco, bajjou.omar@gmail.com.*

³*Faculty of Applied Sciences, Ibn Zohr University, Ait-Melloul, Morocco.*

⁴*UNESCO UNISA Africa Chair in Nanosciences & Nanotechnology (U2ACN2), College of Graduate Studies, University of South Africa (UNISA), Pretoria, South Africa.*

⁵*ERPTM, Faculty of Polydisciplinary Beni Mellal, Sultan Moulay Slimane University, B.P 592, 23000, Beni Mellal-Morocco.*

STUDY on electronic and optical properties of graphene oxide under an external electric field from first-principles

Electronic and optical properties of graphene oxide (GO), under an external electric field (E_{ext}) applied in three directions of space (x, y, z), are investigated using the density functional theory (DFT). The application of the E_{ext} , causes a significant modifications to the electronic and optical properties of GO material. It has change the band gap, total density of states (TDOS), partial density of states (PDOS), absorption coefficient (α), dielectric function, optical conductivity, refractive index and loss function. The band gap of GO layer increases under the effects of the E_{ext} , applied in x and y directions. On the other hand, for z direction, the band gap decreases by the effects of the E_{ext} . The peaks of the TDOS around the Fermi level, change by the E_{ext} applied in (x, y, z) directions. The α peaks of the GO sheet, decreases by the E_{ext} applied in x direction, and increases if E_{ext} applied in y and z directions. It is found that, the electronic and optical properties of GO layer, could be affected by the effects of the E_{ext} and by its direction of application.

Keywords: External electric field, Optical property, First-principle calculation, electronic structure, absorption spectrum.

1. Introduction

Electronic states of graphene derived from π electrons of the carbon atoms, can be calculated using the DFT calculation. In two-dimensional graphene, the carbon atoms form a triangular lattice with the lattice constant $a = \sqrt{3} d_{c-c}$, and the carbon bond length in graphene sheet is $d_{c-c} = 0.142$ nm [1]. A single layer of graphene, the band structure shows zero gap at the K point of the Brillouin zone. This points is also termed Dirac points, which can be opened by the external perturbations such as the application of the E_{ext} or by the strain [2]. Hofmann and Holst proposed a structural model of GO layer, with the epoxy groups (C_2O) only. They supposed that the oxygen functional groups, are bound to the carbon atoms of the hexagon sheet planes [3]. Yan et al. [4,5] studied the arrangement of the epoxy groups on graphene layer, using the first-principles calculations. The epoxy groups are orderly arranged in a chained on the basal plane of graphene, forming specific oxygen-containing groups put on the both sides of graphene sheet.

In several cases, the effects of the E_{ext} can modify the electric current in a semiconductor device [6]. The electric field is simply modifiable in directions. The effects of the E_{ext} adjust the optical response of the 2D graphene. The external dc gates control the Fermi energy and help the photocurrents in graphene material, which are essential for optical modulators and photodetectors, respectively [7]. Therefore, it is very necessary to study the effects of the E_{ext} , on optical and electronic properties of GO. The effects of the E_{ext} has the advantage of being easy to attain and control the physical properties of 2D materials. The E_{ext} applied on electronic and optical properties of GO, have received great attract for fundamental and applied research.

Applying an electric field on materials can cause an electro-optical effects, and change their optical and electronic properties [8,9]. In this paper, the effects of an E_{ext} on electronic structure and optical properties of GO layer, are studied using the first-principles calculations [10]. Including the band gap, density of states and optical properties of GO structure. In the case of applying the E_{ext} on GO layer, a perturbation of electrostatic potential to the Hamiltonian of π -electrons is expected. The effects of an E_{ext} applied in the three directions (x, y, z) of space, modifies the Hamiltonian H of the system as:

$$H = H_0 - eE_x \quad (1)$$

$$H = H_0 - eE_y \quad (2)$$

$$H = H_0 - eE_z \quad (3)$$

Where H_0 is the Hamiltonian of the system without the effects of the E_{ext} .

Our paper is outlined as follows: In section 2, we briefly present the Computational Methods. Section 3 is devoted to discuss the numerical results and give our interpretations. Finally, the conclusions of our study is included in Section 4.

2. Computational methods

The electronic structure simulations and optical properties of the GO model, are calculated based on the DFT calculations. All calculations are performed using the CASTEP code, by the OTFG ultrasoft

pseudopotentials [11,12]. Only the valence electrons (C $2s^22p^2$ and O $2s^22p^4$) are considered using ultrasoft pseudopotentials. The exchange-correlation energy was treated within the generalized gradient approximation (GGA) in the form of Perdew, Burke and Ernzerhof (PBE) functional [13]. A plane-wave energy cut-off was set to 600 eV for all the calculations.

The K-point of the Brillouin zone was sampled using $6 \times 6 \times 1$ gamma-centered Monkhorst-Pack grid during the geometry optimizations of GO [14]. However, during all structural relaxations, the convergence tolerance criteria for the geometry optimization was set to 2×10^{-6} eV/atom for the energy. During the atomic relaxations, the positions of atoms are optimized until the convergence of the force on each atom, was less than 0.003 eV/Å and 0.005 Å for the displacement. The self-consistent field (SCF) convergence tolerance, was set to 2×10^{-6} eV/atom. The internal stress components are less than 0.1 GPa.

In the present simulation, the GO structure is shown in Fig.1. In this model, each O atom forms an epoxy-functional group with two C atoms. In the present work, we have considered that a supercell contains 16 C and 4 O atoms, are coordinates was shown in Table.1. In the atomic structures of the GO layer, four epoxy per 16 C atoms are distributed randomly on both sides of graphene sheet. The effects of the E_{ext} values 0 V/Å, 0.25 V/Å and 0.50 V/Å are applied in (x, y, z) directions, for obtaining the electronic and optical properties of GO. The GO structure was placed inside a unit cell parameters $a= 4.919013$ Å, $b= 8.519982$ Å, $c= 5.614792$ Å and $\alpha= \beta= \gamma= 90^\circ$ for an optimization calculation.

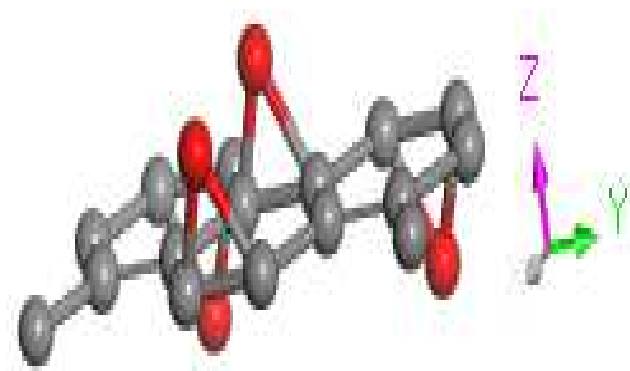


Fig. 1. The crystal structure of GO. The grey sphere represents the carbon atom and the red spheres represents the oxygen atoms.

Table.1: The coordinates of C and O atoms in supercell of GO.

Element	Atom Number	Fractional coordinates of atoms		
		u	v	w
C	1	0.000000	0.166667	0.485553
C	2	0.250000	0.416667	0.485553
C	3	0.000000	0.333333	0.485553
C	4	0.250000	0.083333	0.485553
C	5	0.500000	0.166667	0.485553
C	6	0.750000	0.416667	0.485553
C	7	0.500000	0.333333	0.485553
C	8	0.750000	0.083333	0.485553
C	9	0.000000	0.666667	0.485553
C	10	0.250000	0.916667	0.485553
C	11	0.000000	0.833333	0.485553
C	12	0.250000	0.583333	0.485553
C	13	0.500000	0.666667	0.485553
C	14	0.750000	0.916667	0.485553
C	15	0.500000	0.833333	0.485553
C	16	0.750000	0.583333	0.485553
O	1	0.261226	0.508711	0.729287
O	2	0.768312	0.497341	0.720160
O	3	0.980336	0.727332	0.270713
O	4	0.971581	0.224820	0.274385

3. Results and discussions

3.1 Electronic structure

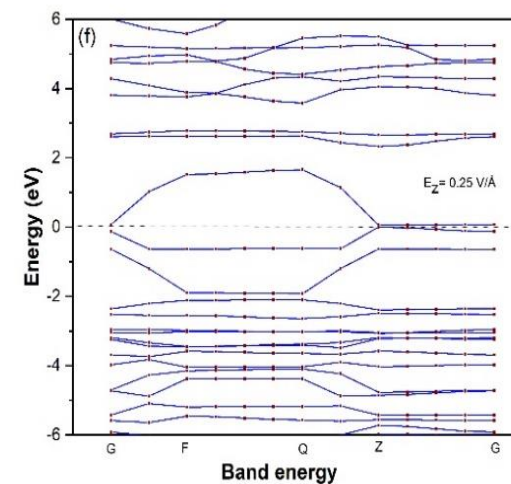
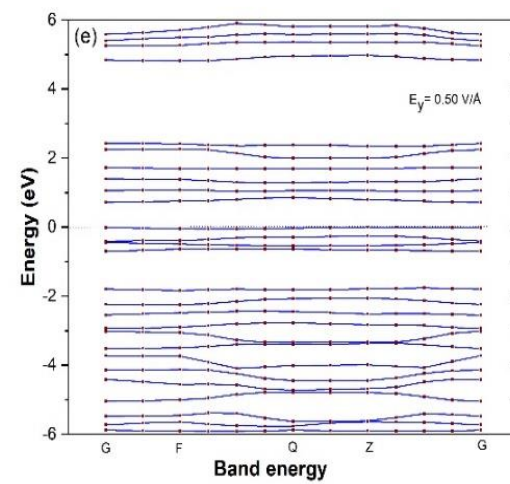
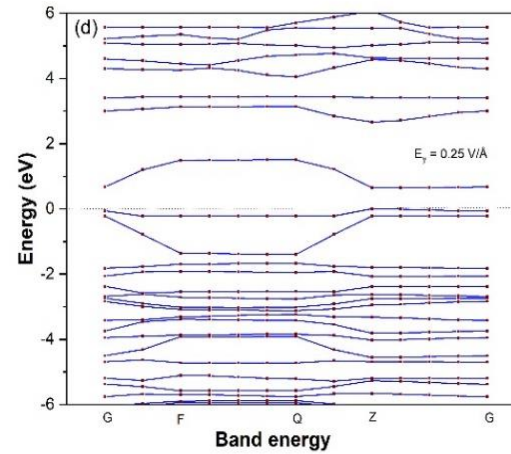
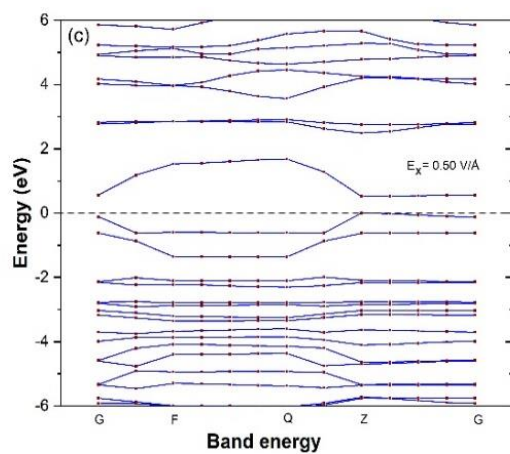
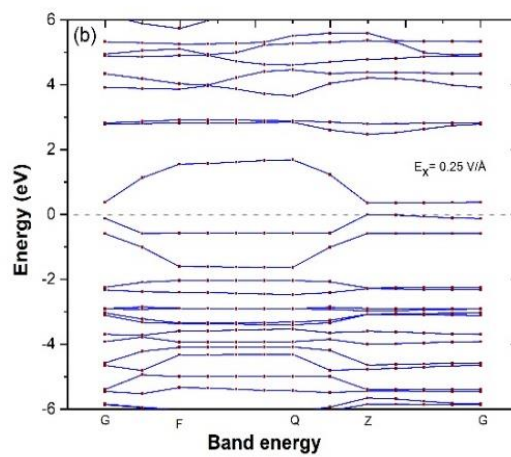
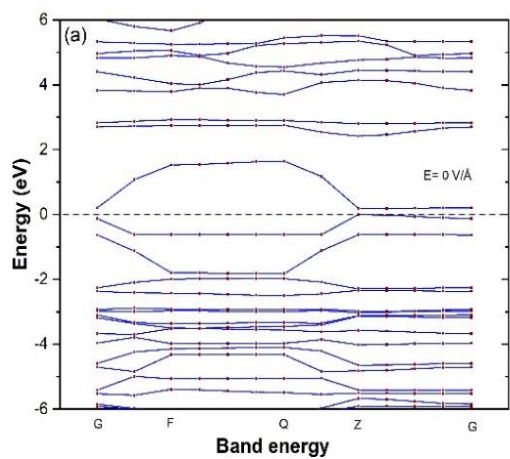
3.1.1 Optical gap

To Applying an E_{ext} is a method to control the energy band gap of 2D-materials. It is very important to know how the electronic band structures are adjusted by the effects of the E_{ext} , applied in (x, y, z) directions of GO layer. The band structures of GO calculated along high symmetry directions of the Brillouin zone, are plotted in Fig.2. The band structures show that the conduction band minimum and the valence band maximum, are located at G and Z points of the Brillouin zone, which indicate that the GO has a direct band gap. In Fig.3, the band gap energy increases from 0.183 eV to 0.522 eV of the E_{ext} values change from 0 V/Å to 0.50 V/Å, respectively, applied on GO sheet in x direction, by reason of the shift upward of conduction band, specifically at Z point of the Brillouin zone. The response of band gap energy of GO to the E_{ext} in x direction, shows a near-linear behavior and facilitates its modulation. In y direction, the band

gap increases from 0.189 eV to 0.719 eV by the effects of the E_{ext} applied on GO from 0 V/Å to 0.50 V/Å respectively. Additionally, an E_{ext} applied on GO sheet from 0 V/Å to 0.50 V/Å in z direction, lead to decreases the band gap energy from 0.183 eV to 0.001 eV respectively, by reason of the shift upward in the valence band, specifically at G point of the Brillouin zone. It can be seen that the E_{ext} lead to shifts the energy levels of GO material, and this displacement is influenced by the direction of its application.

It is clear from Fig.3, that the GO exhibit the modulation of the band gap by the effects of the E_{ext} , applied in (x, y, z) directions of space. Hence, the results of band gap energy indicate the semiconducting properties of GO under the E_{ext} , and become almost metallic for an E_{ext} value equal to 0.50 V/Å applied in z direction. The influence of the E_{ext} on the band gap closer to the Fermi level, can be summarized as follows: For x direction, the conduction band moves upward and the valence band remains almost fixed at Z point of the Brillouin zone. In y direction, the conduction and valence bands move upward for opening the band gap. But for z direction, the conduction band moves downward and the valence band remains almost fixed at Z point of the Brillouin zone, for an E_{ext} value equal to 0.25 V/Å, and the valence band moves upward and the conduction band remains almost fixed at G point of the Brillouin zone, for an E_{ext} value equal to 0.50 V/Å.

The application of a perturbing potential on GO layer, breaks the symmetry and resulting the mixture of its electronic states. The amplitude of the E_{ext} should give rise to a significant modulation of the band gap energy of the GO semiconductor. These results, show an opening and closing of the band gap energy, by reason of the strength of the E_{ext} applied in (x, y) and z directions, respectively. The effect of an E_{ext} is the effective method, to control and modulate the electronic property of GO material. This makes GO a semiconductor with a controllable band gap, which lead to develop the photo detectors devices.



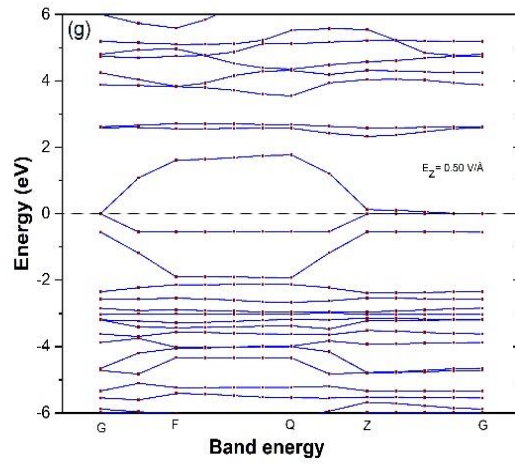


Fig. 2. Band gap energies of GO structure, under an E_{ext} applied in (x, y, z) directions.

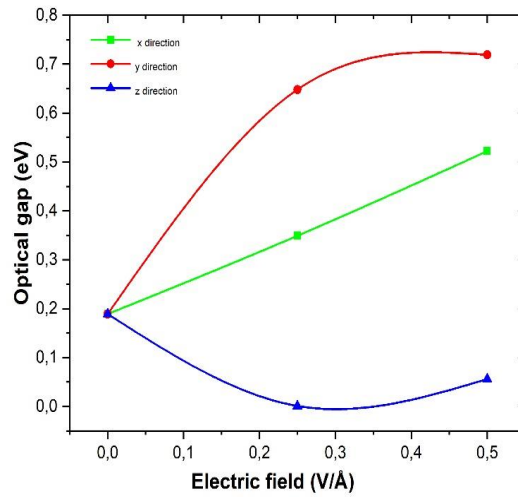


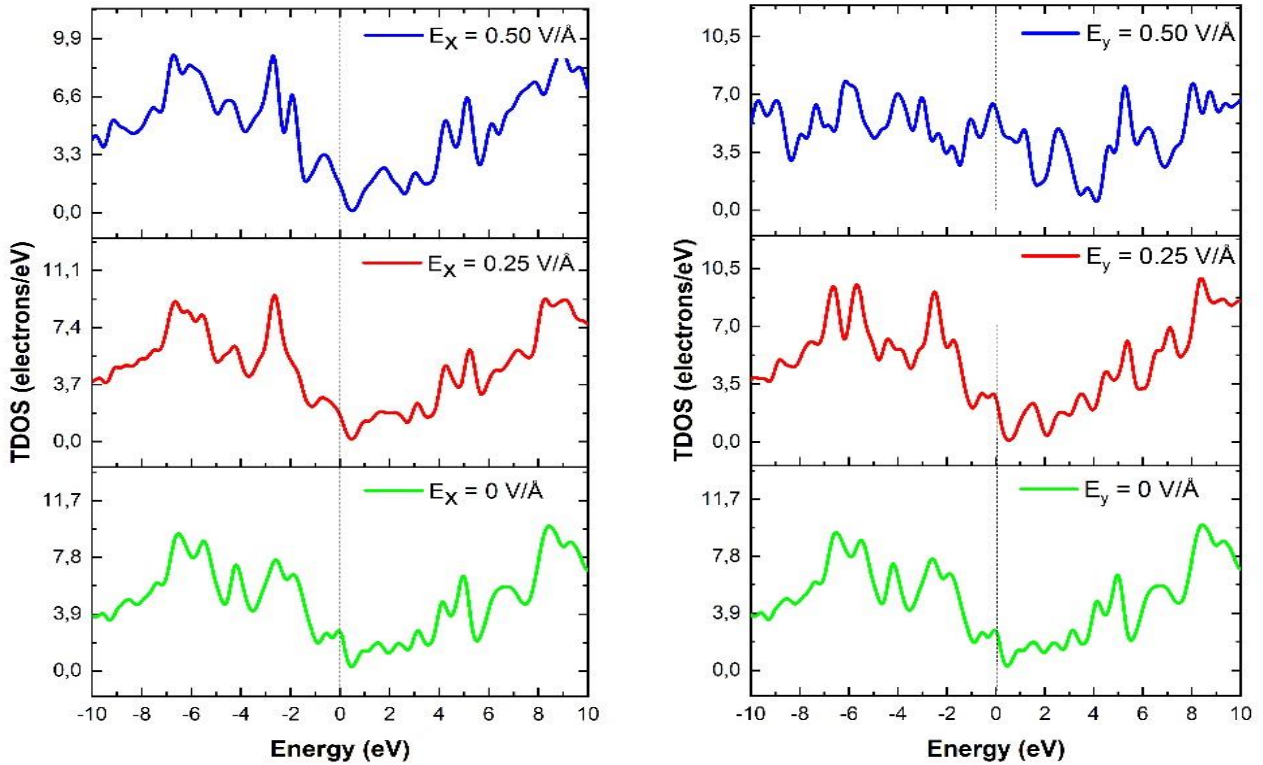
Fig.3. Variation of the band gap as a function of the E_{ext} , applied on GO layer in (x, y, z) directions.

3.1.2 Density of states

The density of states (DOS) is a quantum property, that is used in solid-state physics. It refers to the number of allowed electron energy states per unit energy interval, around an energy E in a solid crystal. In the electronic states, the DOS permits the calculation of the number of electrons for each energy level. Most properties of crystals semiconductors, including their optical and electronic properties are determined by their DOS. The description of these states, defines the electrical conduction properties of a crystal [15]. The total density of states (TDOS) and partial density of states (PDOS) of GO layer, are plotted as a function of

the E_{ext} , as shown in Fig.4 and Fig.5, respectively. The TDOS near the Fermi level exhibits a small population, by reason of the semiconductor character of GO material. The probability of occupation electronic states by the valence electrons, increases around the Fermi level under the effects of the E_{ext} applied in both x and y directions, and decreases by the E_{ext} applied in the z direction of GO layer.

The PDOS, which is essentially the local DOS for each atom in the GO layer, can provide additional insight into any observed changes in the electronic structure. The states of all atoms in GO sheet around the Fermi level, primarily originate from $2p_z$ orbitals and we focused on them for plotted the PDOS. The oxygen atoms loses the electrons while the carbon atoms gains the electrons, under an action of the E_{ext} applied in z direction. The loss of electrons by oxygen atoms comes from O $2p$ orbitals, and the gain of electrons by carbon atoms is attributed to the C $2p$ orbitals under the effects of the E_{ext} . The number of electrons lost by the oxygen atoms or gained by the carbon atoms, increases by the application of the E_{ext} from 0 V/\AA to 0.50 V/\AA in z direction. These results clarify the strong effect of the E_{ext} on the electronic properties of GO material.



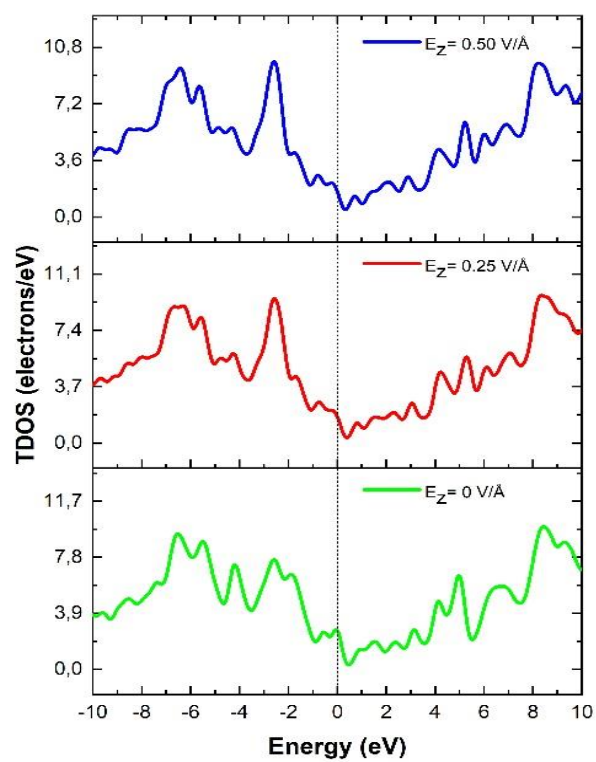


Fig.4. Calculated TDOS as a function of frequency of GO, under an E_{ext} applied in (x, y, z) directions.

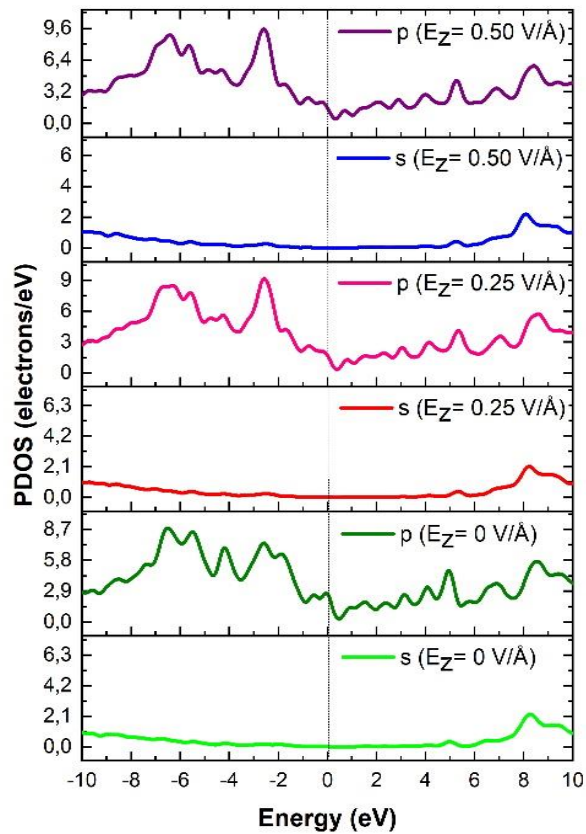
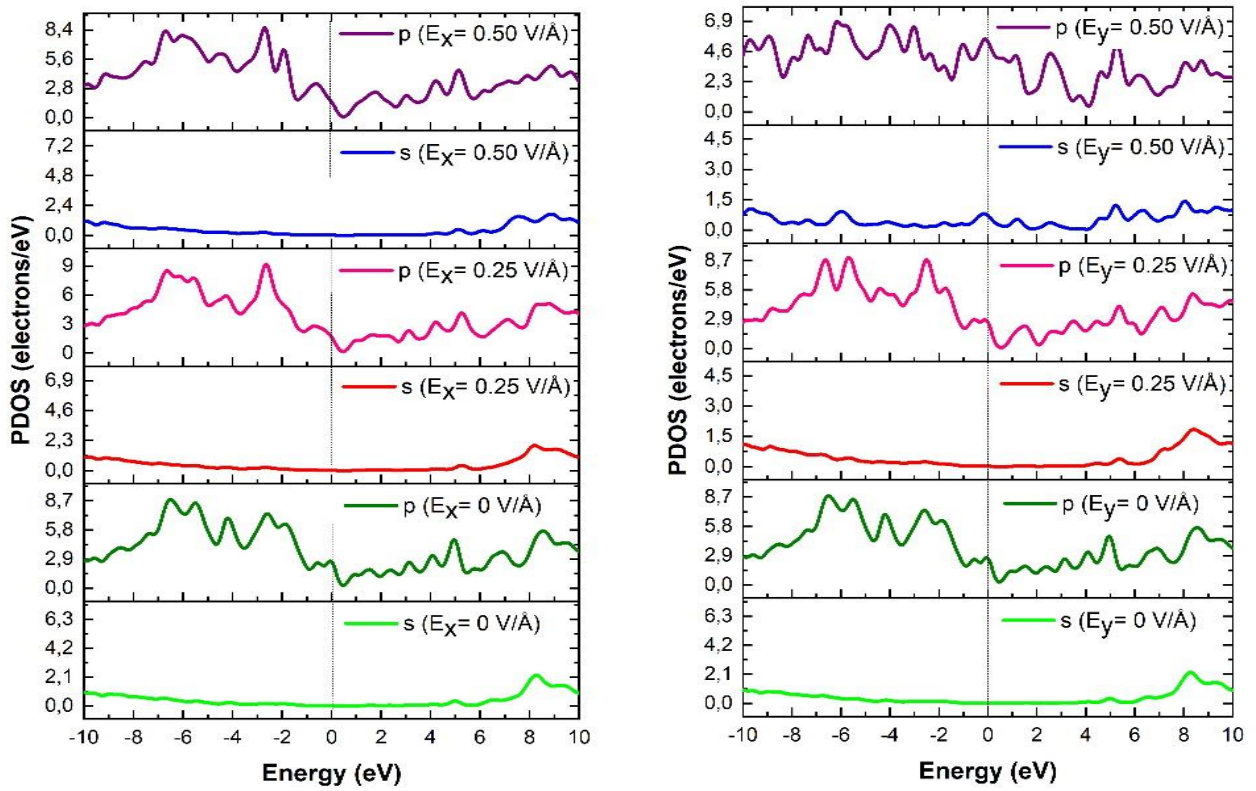


Fig.5. Calculated PDOS as a function of frequency of GO, under an E_{ext} applied in (x, y, z) directions.

3.2 Optical properties

3.2.1 Absorption

In the present study, we have presented the variation of absorption coefficient α as a function of photon energy ($h\nu$), under an E_{ext} from 0 V/Å to 0.50 V/Å, applied in (x, y, z) directions of GO layer in 0 - 8 eV range, as shown in Fig.6. For the absence of an E_{ext} , the absorption spectrum consists of two peaks with different intensities. The first peak with low intensity appear at 3.01 eV, and the second peak identified at 5.69 eV [16]. The source of peaks arises from two essential transitions between electronic states of GO. The first peak corresponds to the transition from occupied n to unoccupied n^* state in the conduction bands. The large second peak corresponds to the transition of π - π^* states for C-C bond in sp^2 hybrid regions. According to these two peaks, GO exhibits a powerful light absorption, it can absorb both ultraviolet and visible light. When the effects of the E_{ext} applied in x direction of GO layer, the intensity of absorption peaks decreases in both ultraviolet and visible ranges, due to the decrease of the number of electrons and photo-generated holes under the E_{ext} effects. In y direction, the E_{ext} applied on GO lead to decrease the intensity of α peaks in the ultraviolet domain, and increase the intensity of α peaks in the visible range. On the other hand, when the E_{ext} applied in z direction, the intensity of α peaks in ultraviolet range increase of 0.25 V/Å, and decrease of 0.5 V/Å. But, in visible range the α peaks increases, due to the decreases of free electrons number in GO sheet Table.2.

The application of the E_{ext} in z direction, leads to increase the redshift of the absorption edge, by reason of the decreases of the band gap energy of GO structure. This result is in agreement with the energy band gap plotted in Fig.3. Finally, these effects demonstrate that the effects of the E_{ext} , can be effectively used to modify the power absorption of light by GO material. The results of our calculations for the absorption spectrum, show that the optical properties of GO, are strongly depend on the direction of applied the E_{ext} . The absorption of visible light by the GO material under an E_{ext} applied in z direction, enables to us increase the light-absorbing capacity, which is essential for photo-induced applications.

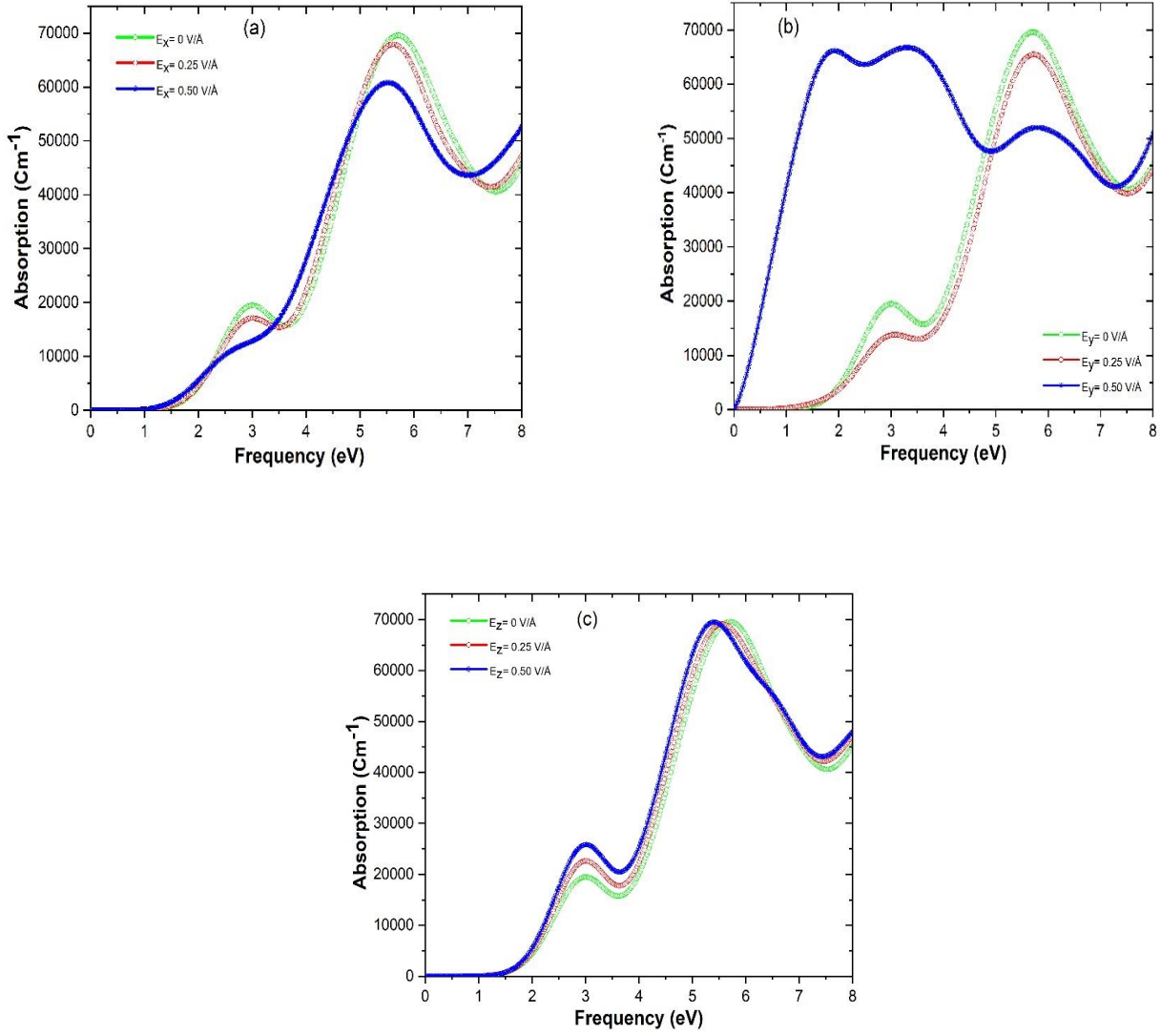


Fig. 6. Calculated $\alpha(\omega)$ of GO structure, under the E_{ext} applied in (x, y, z) directions.

Table 2. The $\alpha(\omega)$ peaks of GO structures under the E_{ext} .

External electric field (V/Å)		$E_x=0$	$E_x=0.25$	$E_x=0.5$	$E_y=0$	$E_y=0.25$	$E_y=0.5$	$E_z=0$	$E_z=0.25$	$E_z=0.5$	
$\alpha(\omega)$	First peak	Peak position (eV)	3.01	3.00	x	3.01	3.06	1.91	3.01	3.00	3.01
		Maximum peak (Cm ⁻¹)	19461.14	17093.05	x	19461.14	13799.92	66149.64	19461.14	22615.11	25830.64
	Second peak	Peak position (eV)	5.69	5.61	5.52	5.69	5.71	3.30	5.69	5.55	5.40
		Maximum peak (Cm ⁻¹)	69570.62	67897.81	60782.58	69570.62	65472.32	66729.98	69570.62	69117.66	69490.79

3.3.2 Dielectric function

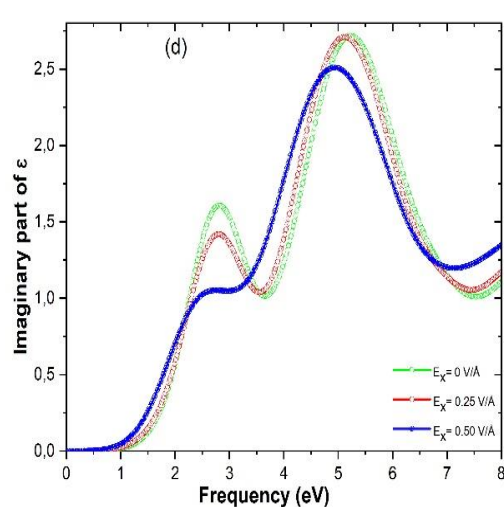
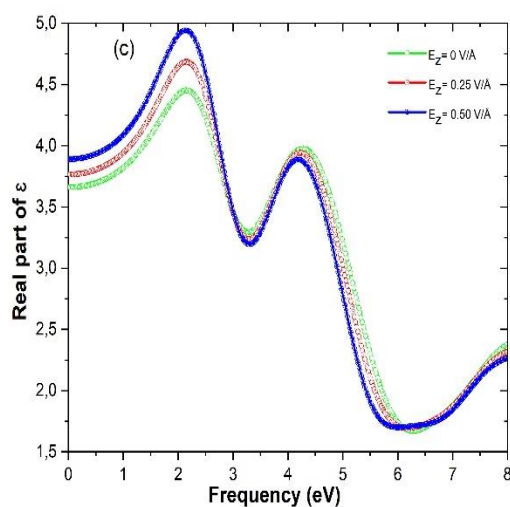
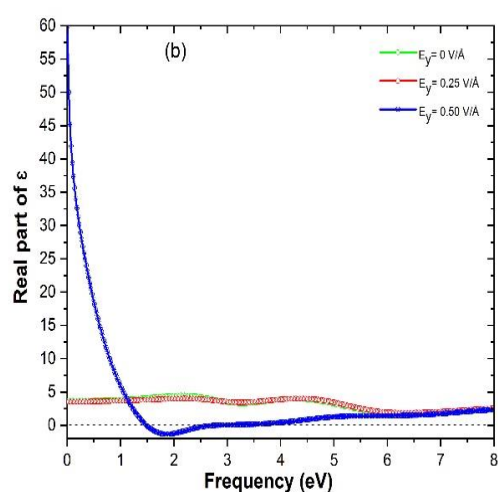
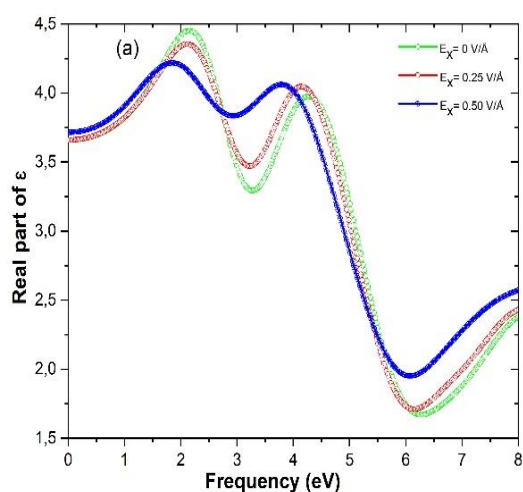
The complex frequency-dependent dielectric function, $\varepsilon(\omega)$ can be used to describe the optical properties of 2D-material, and describes how light interacts when propagating through matter. It determines the dispersion effects by its real part, $\varepsilon_1(\omega)$ and the absorption effects by the imaginary part, $\varepsilon_2(\omega)$. We measured the energy dependence of GO dielectric function, under the E_{ext} applied in (x, y, z) directions. The complex dielectric function $\varepsilon(\omega)$ is the sum of real and imaginary parts:

$$\varepsilon(\omega) = \varepsilon_1(\omega) + i\varepsilon_2(\omega) \quad (4)$$

In the present study, the real and imaginary parts of the GO dielectric function, are calculated in absence and presence of the effects of the E_{ext} , applied in (x, y, z) directions in 0 - 8 eV range, as presented in Fig.7. At low energies, $\varepsilon(\omega)$ is associated with electronic intraband transitions inside the conduction band. In this spectral range, the optical response is dominated by the free electron behavior. At higher energies, $\varepsilon(\omega)$ reflects the electronic interband transitions. For the E_{ext} increases in x direction of GO layer, the peaks of $\varepsilon_1(\omega)$ are increase in UV domain and decrease in visible range, which interprets the minimization of the decomposition of visible light in monochromatic radiations. The peaks concerning the imaginary part $\varepsilon_2(\omega)$ are decrease in both UV and visible ranges, under the E_{ext} , and these peaks are towards to redshifted. For y direction, the peaks of $\varepsilon_1(\omega)$ decrease in both UV and visible ranges, under the effects of the E_{ext} , which interprets the decrease of the dispersion of incident light inside GO material. The peaks which concerning $\varepsilon_2(\omega)$, decrease for the UV and increase in visible ranges, under the E_{ext} . Additionally, for z direction the peaks of $\varepsilon_1(\omega)$ decrease in UV range and increase in visible domain, under the E_{ext} , which interprets the increase dispersion of visible light. On the other hand, the peaks of $\varepsilon_2(\omega)$ increase in both UV and visible domains under the E_{ext} . These results of $\varepsilon_2(\omega)$ part, shows the remarkable enhanced abilities to absorb photons by GO material, under the E_{ext} applied in z direction for the visible area Table.3.

The difference between $\varepsilon_1(\omega)$ values in (x, y, z) directions, suggests that an anisotropic behavior of the optical properties of GO material, under the E_{ext} . For an E_{ext} applied in both x and z directions of GO structure, $\varepsilon_2(\omega)$ has two peaks in 2-8 eV range, are always related to the electron excitation. The $\varepsilon_2(\omega)$

part, has a low value for the incident photons has the energy ($E = h\nu$) less than 2 eV Fig.7. In addition, it is noteworthy to say that the value of $\varepsilon_1(\omega) > 0$ and $\varepsilon_2(\omega) = 0$ in 0-1 eV range, means that this region transparent. It means that there is no absorption at low energy, because in this case the valence electrons of GO layer, cannot react fast with the E_{ext} , and the transition between the valence band maximum and the conduction band minimum or between the orbitals is forbidden. Then, under an E_{ext} , GO material is an absorbent material for a wide range of energy, which indicates that this material can be used as an important element in several optoelectronic devices, such as the transparent conducting films and photovoltaic devices.



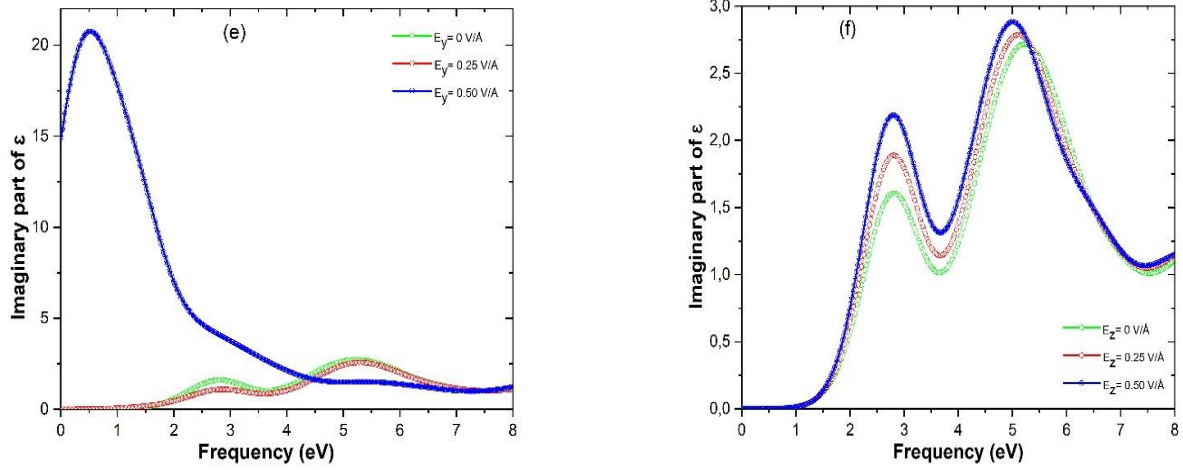


Fig. 7. Calculated $\epsilon(\omega)$ of GO structure, under the E_{ext} applied in (x, y, z) directions.

Table 3. The $\epsilon(\omega)$ peaks of GO layer, under the E_{ext} .

External electric field (V/Å)		$E_x=0$	$E_x=0.25$	$E_x=0.5$	$E_y=0$	$E_y=0.25$	$E_y=0.5$	$E_z=0$	$E_z=0.25$	$E_z=0.5$	
$\epsilon_1(\omega)$	First peak	Peak position (eV)	2.13	2.12	1.84	2.15	2.18	1.86	2.13	2.14	2.14
		Maximum peak	4.44	4.35	4.21	4.45	4.00	-1.33	4.44	4.68	4.94
	Second peak	Peak position (eV)	4.28	4.14	3.79	4.28	4.35	x	4.28	4.22	4.18
		Maximum peak	3.97	4.04	4.06	3.97	3.99	x	3.97	3.94	3.88
$\epsilon_2(\omega)$	First peak	Peak position (eV)	2.82	2.81	2.75	2.82	2.87	0.53	2.82	2.81	2.80
		Maximum peak	1.60	1.41	1.05	1.60	1.09	20.75	1.60	1.88	2.18
	Second peak	Peak position (eV)	5.22	5.11	4.94	5.22	5.28	5.36	5.22	5.12	4.99
		Maximum peak	2.71	2.70	2.50	2.71	2.57	1.51	2.71	2.78	2.88

3.3.3 Refractive index

Propagation in absorbing materials, can be described by the complex-valued of the refractive index $n^*(\omega)$.

The imaginary part $k(\omega)$ of $n^*(\omega)$ then handles the attenuation, while the real part $n(\omega)$ accounts for the refraction by [17]:

$$n^*(\omega) = n(\omega) + ik(\omega) \quad (5)$$

$$n(\omega) = \sqrt{\frac{|\epsilon(\omega)| + \epsilon_1(\omega)}{2}} \quad (6)$$

$$k(\omega) = \sqrt{\frac{|\varepsilon(\omega)| - \varepsilon_1(\omega)}{2}} \quad (7)$$

The variation of $n(\omega)$ and $k(\omega)$ of GO layer, under the effects of the E_{ext} from 0 V/Å to 0.50 V/Å, applied in (x, y, z) directions in terms of frequency, are found using the CASTEP code and depicted in Fig.8. The above values of $\varepsilon_1(0)$ and $n(0)$ validate the relation $n = \sqrt{\varepsilon_1}$ Table.4.

The real part $n(\omega)$ of GO layer, under the E_{ext} varies as a function of the frequency, which indicate that the GO material is a dispersive medium. The dispersion of light inside GO sheet, is influenced by the effects of the E_{ext} and its direction of application. The $n(\omega)$ part value is greater than 1.126. In x direction, $n(\omega)$ decreases in the visible range and increases in the UV region, under the application of the E_{ext} , by reason of the change of light velocity ($v = \frac{c}{n}$) inside the GO sheet. The peaks of $k(\omega)$ part, decreases in both visible and UV ranges, by reason of the decrease of the absorption light under the E_{ext} . The application of the E_{ext} on the GO layer in y direction, lead to decrease $n(\omega)$ part in both visible and UV ranges, and increase $k(\omega)$ part in visible range. For z direction, the $n(\omega)$ part increases in the visible range, because the application of E_{ext} , lead to increase the interaction and collision between incident photons and particles inside GO layer. In addition, the $k(\omega)$ part increases in both ultraviolet and visible regions, by reason of the decrease of band gap energy under the E_{ext} applied in z direction Table.5 and Fig.8. When we analyse the graphs of $\varepsilon_2(\omega)$ and $k(\omega)$ parts, a similar physical behavior is observed in Fig.7 and Fig.8. These results give the information's of the absorption light by GO material.

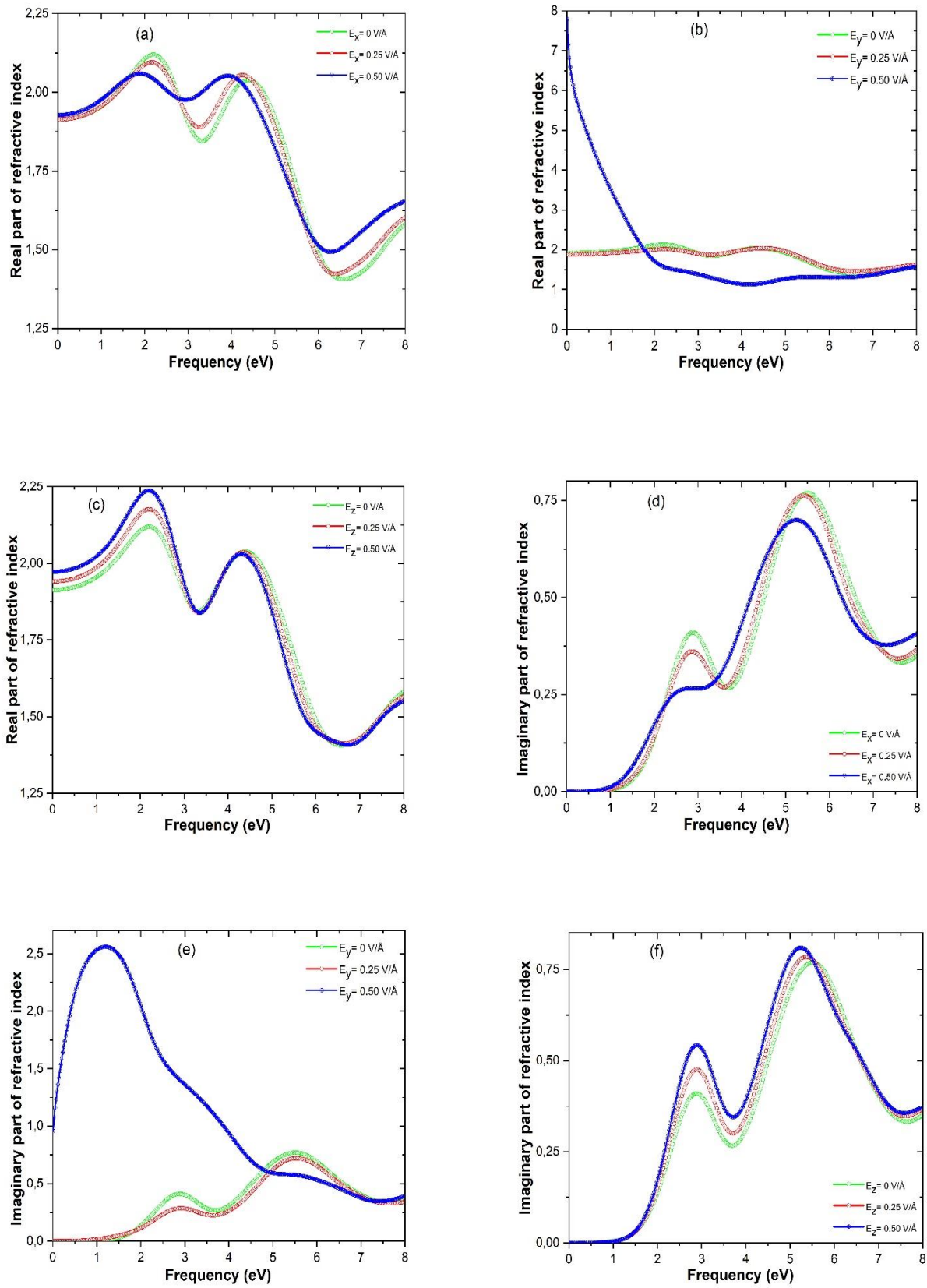


Fig. 8. Calculated $n^*(\omega)$ of GO layer, under the E_{ext} applied in (x, y, z) directions.

Table. 4. The static dielectric constant $\epsilon_1(0)$ and the static refractive index $n(0)$ of GO layer.

Parameters	E_x			E_y			E_z		
E (V/Å)	0	0.25	0.50	0	0.25	0.50	0	0.25	0.50
$n(0)$	1.91	1.91	1.93	1.91	1.87	7.79	1.91	1.94	1.97
$\epsilon_1(0)$	3.66	3.66	3.72	3.66	3.52	59.88	3.66	3.77	3.89

Table. 5. The peaks of real and imaginary parts of $n^*(\omega)$ of GO sheet.

External electric field (V/Å)		$E_x=0$	$E_x=0.25$	$E_x=0.5$	$E_y=0$	$E_y=0.25$	$E_y=0.5$	$E_z=0$	$E_z=0.25$	$E_z=0.5$	
$n(\omega)$	First peak	Peak position (eV)	2.19	2.16	1.89	2.19	2.22	x	2.19	2.21	2.18
		Maximum peak	2.11	2.09	2.05	2.11	2.00	x	2.11	2.17	2.23
	Second peak	Peak position (eV)	4.38	4.25	3.92	4.38	4.48	5.49	4.38	4.35	4.29
		Maximum peak	2.03	2.05	2.05	2.03	2.03	1.31	2.03	2.03	2.02
$k(\omega)$	First peak	Peak position (eV)	2.88	2.85	2.82	2.88	2.91	1.19	2.88	2.89	2.88
		Maximum peak	0.40	0.36	0.26	0.40	0.28	2.55	0.40	0.47	0.54
	Second peak	Peak position (eV)	5.50	5.41	5.24	5.50	5.54	x	5.50	5.38	5.25
		Maximum peak	0.76	0.76	0.69	0.76	0.72	x	0.76	0.78	0.80

3.3.4 Conductivity

It is interesting to know the complex optical conductivity $\sigma(\omega)$ of GO material, because we can derive valuable physic information's from it. The parts of $\sigma(\omega)$ are given by the following relation [18]:

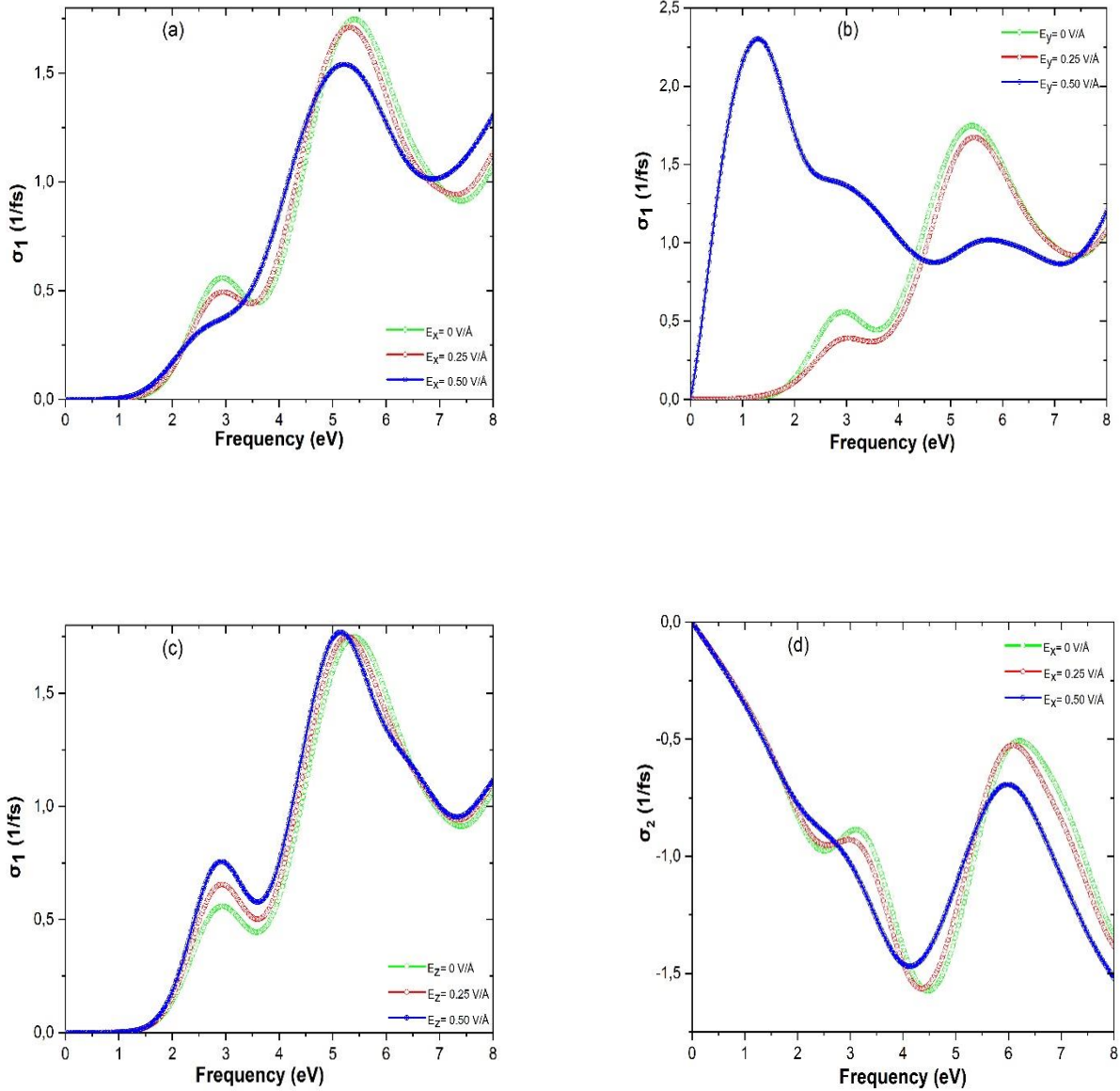
$$\sigma(\omega) = \sigma_1(\omega) + i\sigma_2(\omega) \quad (8)$$

$$\sigma_1(\omega) = 2nk \left(\frac{\omega}{4\pi} \right) \quad (9)$$

$$\sigma_2(\omega) = [1 - (n^2 - k^2)] \left(\frac{\omega}{4\pi} \right) \quad (10)$$

Optical conductivity was calculated of GO layer under the effects of the E_{ext} , applied in (x, y, z) directions. The $\sigma_1(\omega)$ and $\sigma_2(\omega)$ parts as a function of frequency are plotted in Fig.9. In the case of the absence the E_{ext} , the peak of $\sigma_1(\omega)$ at 5.41 eV corresponds to the fundamental band gap, by reason of the interband transitions. In x and y directions, the peaks of $\sigma_1(\omega)$ and $\sigma_2(\omega)$ parts are decreases by the effects of the E_{ext} in both UV and visible ranges, by reason of the increase of the band gap energy. On the other hand, the application of the E_{ext} on GO layer in z direction, lead to increase the peaks of $\sigma_1(\omega)$ and $\sigma_2(\omega)$ parts in both UV and visible ranges, by reason of the decrease of the band gap energy Table.6. In (x, z)

directions, $\sigma_2(\omega)$ has a negative value in 0-8 eV range, which indicates that the charge is well-distributed in GO layer Fig.9. Additionally, in (x, z) directions, its noteworthy to say $\sigma_1(\omega) = 0 \frac{1}{fs}$ in 0-1 eV range, by reason of no absorption at low frequency, because the E_{ext} cannot react with the valence electrons inside the GO structure. The Fermi level can be identified by the local minimum of $\sigma_2(\omega)$ part. The application of the E_{ext} on GO layer therefore pushes the Fermi level, relative to the Dirac point of the Brillouin zone. Although, it has been reported that the effects of the E_{ext} on GO structure, can modify the position and the shape of the van Hove singularity peaks in the visible range.



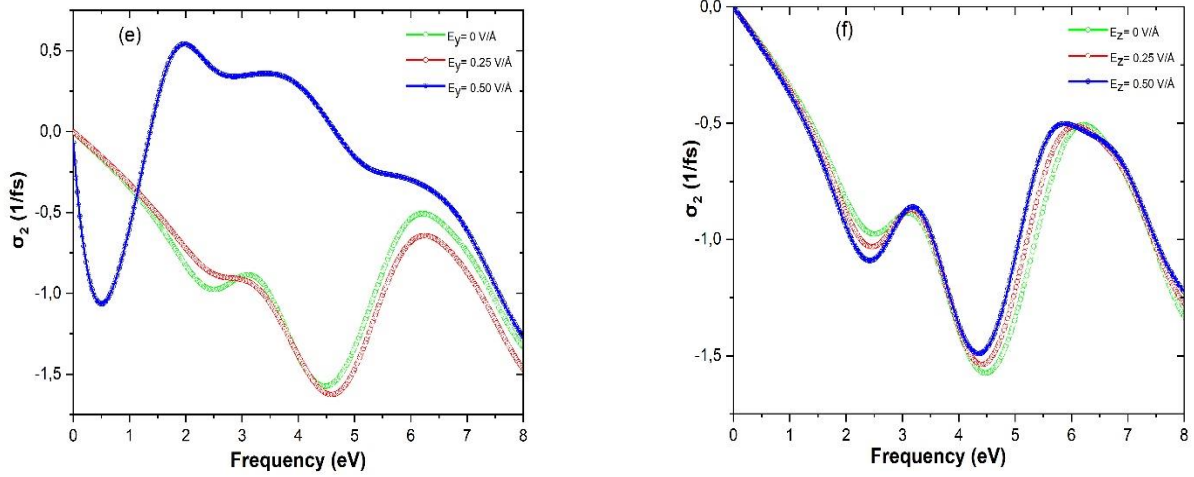


Fig. 9. Calculated $\sigma(\omega)$ of GO structure, under the E_{ext} applied in (x, y, z) directions.

Table. 6. The peaks of real and imaginary parts $\sigma(\omega)$ of the GO layer under the E_{ext} .

External electric field (V/Å)		$E_x=0$	$E_x=0.25$	$E_x=0.50$	$E_y=0$	$E_y=0.25$	$E_y=0.50$	$E_z=0$	$E_z=0.25$	$E_z=0.5$	
$\sigma_1(\omega)$	First peak	Peak position (eV)	2.92	2.94	x	2.92	3.02	1.29	2.92	2.92	2.90
		Maximum peak (1/fs)	0.55	0.49	x	0.55	0.39	2.30	0.55	0.65	0.75
	Second peak	Peak position (eV)	5.41	5.31	5.22	5.41	5.45	5.73	5.41	5.27	5.14
		Maximum peak (1/fs)	1.74	1.71	1.54	1.74	1.67	1.01	1.74	1.74	1.76
$\sigma_2(\omega)$	First peak	Peak position (eV)	3.10	2.98	X	3.10	X	1.97	3.10	3.15	3.18
		Maximum peak (1/fs)	-0.88	-0.92	X	-0.88	X	0.54	-0.88	-0.87	-0.86
	Second peak	Peak position (eV)	6.21	6.08	5.98	6.21	6.25	3.41	6.21	6.08	5.87
		Maximum peak (1/fs)	-0.50	-0.52	-0.69	-0.50	-0.64	0.35	-0.50	-0.51	-0.50

3.3.5 Loss function

The electron loss function $L(\omega)$ describes the energy loss of a fast electron traversing a material, with the change of frequency. From the real and imaginary parts of $\epsilon(\omega)$, the energy loss function can easily be obtained by [19]:

$$L(\omega) = -Im\left(\frac{1}{\epsilon(\omega)}\right) = \frac{\epsilon_2(\omega)}{\epsilon_1^2(\omega) + \epsilon_2^2(\omega)} \quad (11)$$

The $L(\omega)$ of GO layer under the E_{ext} applied in (x, y, z) directions, shown in Fig.10. The origin of $L(\omega)$ peaks in 0-8 eV range, due to the collective excitations at various photon energies. The $L(\omega)$ exhibits two peaks approximately at 3 and 6 eV, which are associated with the plasma frequency. These two peaks

indicate the maximum energy lost in GO sheet, under the effects of the E_{ext} . The application of the E_{ext} on GO layer in x direction, lead to decrease the peaks of $L(\omega)$ in both visible and UV ranges. On the other hand, the effect of an $E_{ext} = 0.25 \text{ V/\AA}$ applied on GO sheet in y direction, lead to decrease the peaks of $L(\omega)$ in both visible and UV ranges. But, the effect of an $E_{ext} = 0.50 \text{ V/\AA}$ lead to increase the peaks of $L(\omega)$ in both visible and UV ranges. Additionally, the application of the E_{ext} on GO in z direction, lead to increase the first peaks of $L(\omega)$ in visible range, by reason of the increase the scattering between the incident visible light and the different particles inside GO structure Table.7. The peaks at 6 eV, due to the energy lost for π electrons and the peaks at 3 eV are due to the energy lost for π and σ electrons in GO layer, under an E_{ext} effects. A peak in the $L(\omega)$ corresponds to a dip in the $\epsilon_1(\omega)$ part, as shown in Fig.7 and Fig.10.

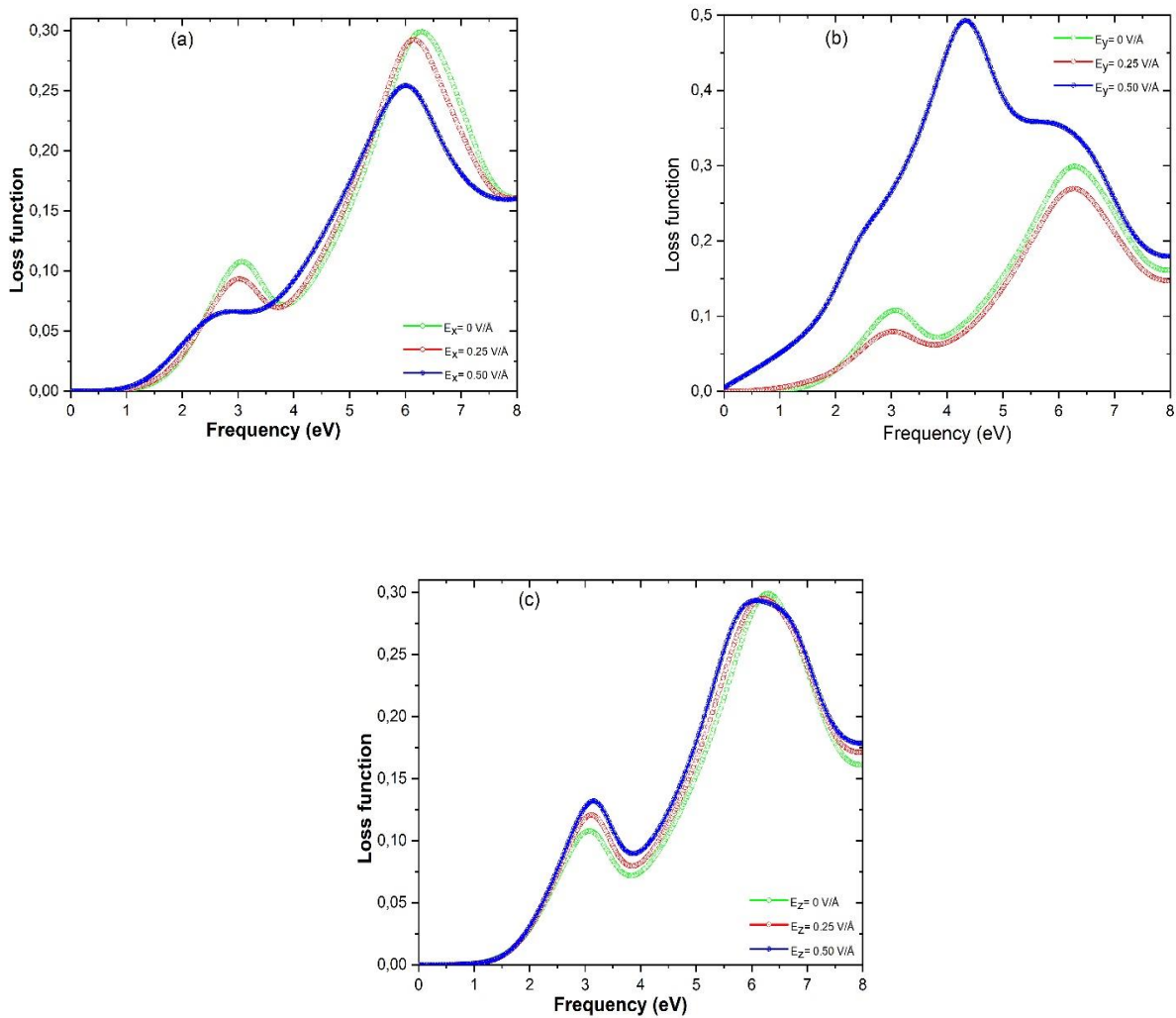


Fig. 10. Calculated $L(\omega)$ of GO structure, under the E_{ext} applied in (x, y, z) directions.

Table. 7. The $L(\omega)$ peaks of GO layer, under the E_{ext} applied in (x, y, z) directions.

External electric field (V/Å)		$E_x=0$	$E_x=0.25$	$E_x=0.5$	$E_y=0$	$E_y=0.25$	$E_y=0.5$	$E_z=0$	$E_z=0.25$	$E_z=0.5$	
$L(\omega)$	First peak	Peak position (eV)	3.07	3.02	2.73	3.07	3.04	4.33	3.07	3.13	3.16
		Maximum peak	0.10	0.09	0.06	0.10	0.07	0.49	0.10	0.12	0.13
	Second peak	Peak position (eV)	6.29	6.15	6.00	6.29	6.27	x	6.29	6.19	6.08
		Maximum peak	0.29	0.29	0.25	0.29	0.26	x	0.29	0.29	0.29

4 Conclusions

To conclude, we have studied the electronic and optical properties of GO layer, under the effects of the E_{ext} by using the DFT calculations. The application of the E_{ext} on GO sheet in (x, y, z) directions, produces different modifications in the band structures and optical properties. We have shown that the GO is a semiconductor material, and its band gap can be significantly modulate by applying an E_{ext} in the three direction of space (x, y, z). We observed the changes of the dielectric function and the absorption peaks, by reason of the modification of the band gap energy under the E_{ext} . These insights provide a basis for the applications of GO material under the effects of the E_{ext} in optoelectronic devices.

Acknowledgement

In conclusion, the authors sincerely thank all that contributed to this scientific work and particularly Sultan Moulay Slimane University.

Contribution statement

The authors have approved the manuscript and agree with submission to your esteemed journal. There are no conflicts of interest to declare. All authors have participated in (a) conception and design, or analysis and interpretation of the data; (b) drafting the article or revising it critically for important intellectual content; and (c) approval of the final version.

References

- [1] V. Lukose, R. Shankar, G. Baskaran, Phys. Rev. Lett. 98 (2007).
- [2] R. Balu, X. Zhong, R. Pandey, S.P. Karna, Appl. Phys. Lett. 100 (2012) 3–6.

- [3] J. Zhao, L. Liu, F. Li, *Structural Modeling and Physical Properties*, (2015) 31–56.
- [4] J.A. Yan, L. Xian, M.Y. Chou, *Phys. Rev. Lett.* 103 (2009).
- [5] J.A. Yan, M.Y. Chou, *Phys. Rev. B - Condens. Matter Mater. Phys.* 82 (2010) 21–24.
- [6] S. Ganguly, J.J. Ghosh, *Indian J. Biochem. Biophys.* 16 (1979) 61–65.
- [7] F. Bonabi, T.G. Pedersen, *Phys. Rev. B.* 99 (2019).
- [8] D. Singh, S.K. Gupta, I. Lukačević, M. Mužević, Y. Sonvane, R. Ahuja, *Sci. Rep.* 9 (2019) 1–12.
- [9] Y. Li, J. Chen, C. Zhao, *RSC Adv.* 7 (2017) 56676–56681.
- [10] S. Nigam, S.K. Gupta, C. Majumder, R. Pandey, *Phys. Chem. Chem. Phys.* 17 (2015) 11324–11328.
- [11] B. Delley, *J. Chem. Phys.* 92 (1990) 508–517.
- [12] E.R. McNellis, J. Meyer, K. Reuter, *Phys. Rev. B - Condens. Matter Mater. Phys.* 80 (2009).
- [13] J.P. Perdew, K. Burke, M. Ernzerhof, *Phys. Rev. Lett.* 77 (1996) 3865–3868.
- [14] Hendrik J Monkhorst, J.D. Pack, *Phys. Rev. B.* 13 (1976) 5188–5192.
- [15] R. Marchiori, Elsevier Inc., 2017.
- [16] P. Johari, V.B. Shenoy, *ACS Nano.* 5 (2011) 7640–7647.
- [17] H. Lashgari, A. Boochani, A. Shekaari, S. Solaymani, *Appl. Surf. Sci.* 369 (2016) 76–81.
- [18] P. Gravier, M. Sigrist, G. Chassaing, *Opt. Acta (Lond).* 24 (1977) 733–741.
- [19] E.A. Taft, H.R. Philipp, *Phys. Rev.* 138 (1965).